engineering proceedings

MDPI

Proceeding Paper

Diagnosis of Incipient Faults in Induction Motors Using Clarke, Park, and FFT Transforms with IQRTukey Statistical Filtering and a Random Forest Classifier †

Andrés Villagrán, Martín Peralta, Esteban Yajamin and William Oñate *

Carrera en Electrónica y Automatización, Universidad Politécnica Salesiana (UPS), Quito 170146, Ecuador; avillagrans@est.ups.edu.ec (A.V.); mperaltap1@est.ups.edu.ec (M.P.); myajaminr@est.ups.edu.ec (E.Y.)

* Correspondence: wonate@ups.edu.ec; Tel.: +593-989-325-276

† Presented at the International Conference on Electronics, Engineering Physics and Earth Science (EEPES2026), Bandirma, Turkey, 24–27 June 2026.

Abstract

Today's manufacturing industries require a continuous process free of unexpected downtime on their production lines. In light of this, this study proposes an innovative method for the early diagnosis of faults in three-phase induction motors that incorporates various mathematical transforms (Clarke, Park, and FFT) and statistical tools (interquartile range (IQR) and Tukey's method). This method enables the cleaning and normalization of a dataset that serves as the input for a Random Forest Classifier ML model. By setting an IQR of ±1.5, over 97% accuracy is achieved across all classes (Loop CC, Bearing, Broken Bar, and Optimal), resulting in an overall accuracy of 98.25%.

Keywords: incipient faults; induction motor; Clarke transform; Park transform; FFT (fast Fourier transform); IQR (interquartile range); Tukey's test; random forest classifier

1. Introduction

The efficiency and optimal performance of three-phase induction motors are critical factors in numerous industrial and commercial applications. Any failure in these motors can result in significant losses for the industry. Consequently, methods for diagnosing and detecting faults in three-phase induction motors are a significant area of interest for implementing predictive maintenance strategies, enabling intervention before the motor fails and thereby reducing costs and downtime.

Traditionally, fault identification has been carried out through visual inspections [1] of the current waveform (MSCA) and motor voltage analysis (MVSA) [2], vibration analysis and temperature measurements [3,4]. However, these methods tend to be reactive and do not always allow for an accurate diagnosis.

Modern studies, on the other hand, employ various types of mathematical transforms such as Fourier, Wavelet, Clarke, Park and Hilbert, with [5,6] specifying that the Park transform is a useful tool for the analysis of electrical signals and the identification of anomalous patterns that may indicate incipient faults in synchronous and asynchronous motors. Conversely, ref. [7] notes that this type of study does not yield a reliable interpretation of the results and tends to focus on a single fault type, failing to adopt a holistic approach encompassing multiple defect types. For its part, ref. [8] clarifies that fault diagnostics could be improved if there is synergy between the results of mathematical transforms and statistical analysis, such as standard deviation or the correlation coefficient. Thus, ref. [9]

Check for updates

Academic Editors: Teodor Iliev, Ivaylo Stoyanov, Grigor Mihaylov and Selahattin Kosunalp

Published: 10 September 2026

Copyright: © 2026 by the authors. Licensee MDPI, Basel, Switzerland. This article is an open access article distributed under the terms and conditions of the Creative Commons Attribution (CC BY) license.

proposes the transformation and decomposition of three-phase currents using Park and an independent component analysis (ICA) algorithm, respectively; they refer to this result, which associates irregularities in the rotor and stator, as MSCA and use statistical indicators for its classification.

On the other hand, combining the methods mentioned earlier with artificial intelligence (AI) techniques has proven effective for fault classification; however, these approaches also need intensive processing and detailed analysis of input data [10]. Therefore, ref. [11] performs a time-frequency analysis (STFT) of the stator currents and a statistical analysis of infrared thermograms, classifying faults such as mechanical misalignment, imbalance, bearings, and rotor bars—using SVM/KNN. Meanwhile, ref. [12] uses the Discrete Wavelet Transform (DWT) and the Partitioning Around Medoids (PAM) clustering algorithm to detect defects in inner and outer raceway bearings. Similarly, ref. [13] combines the Clarke and Park transforms with an RGB image encoding method, using the resulting data as input to a CNN-based machine learning model to identify effects of inter-turn short circuits (ITSC). Likewise, ref. [14] detects ITSC faults and the affected phase by using the spatial vector of stator currents as input data for ML models such as Random Forests (RF), Support Vector Machines (SVM), k-Nearest Neighbors (KNN), feedforward neural networks (FNN), and recurrent neural networks (RNN).

Based on the above, this study provides a methodology to classify four types of conditions detectable in induction motors, such as healthy condition and incipient faults (bearings, short circuits in the coil loop, and broken bars). This process uses a combination of three types of transforms (Clarke-Park-FFT) and statistical adjustment based on the interquartile range (IQR), which allows for data cleaning during pre-processing and also improves prediction accuracy during the validation of the detection system.

This document is organized as follows: Section 1 provides the introduction; Section 2 covers the materials and methods; Section 3 presents the results; Section 4 contains the discussion; and Section 5 outlines the study's conclusions.

2. Materials and Methods

The block diagram shown in Figure 1 consists of two stages: the first involves processing and extracting motor characteristics, and the second concerns modelling and validating the ML model. The internal processes are carried out sequentially; that is, the first part involves supervised data acquisition, which is performed using a K&H MFG test bench module. This includes a dynamometer (see Table 1) comprising a motor with a magnetic brake controlled by a closed-loop control system, current transducers, differential signal amplifiers, voltage and current measurement equipment, an external storage device, WEG W22 motors (see Table 1) and a GW Instek GDS-2102A oscilloscope with 100 MHz bandwidth and a maximum sampling rate of 2 GS/s, configured to a time base of 100 ms/division, which allows spectra to be obtained at 1 Hz intervals within a range of 0–1 kHz. In the second part, the analyses are simplified and fault patterns are highlighted; using the Clarke transform, the demodulation of the stator currents i_a, i_b, i_c is applied to obtain a stationary frame consisting of two orthogonal components and their angles Alpha (α) and Beta (β). Subsequently, the components i_α and i_β are taken and projected onto a rotating frame synchronised with the air-gap magnetic field, thereby identifying any variation in the currents i_d and i_q that correspond to magnetisation and torque, respectively. In the third part, the FFT is used to represent the results in the frequency-amplitude domain as spectral content. For the final part, in a Python IDE (Spyder v5.4.3), statistical methods are applied to ensure data cleaning and robustness and to identify deviations indicative of faults.

https://doi.org/10.3390/engproc2026154077

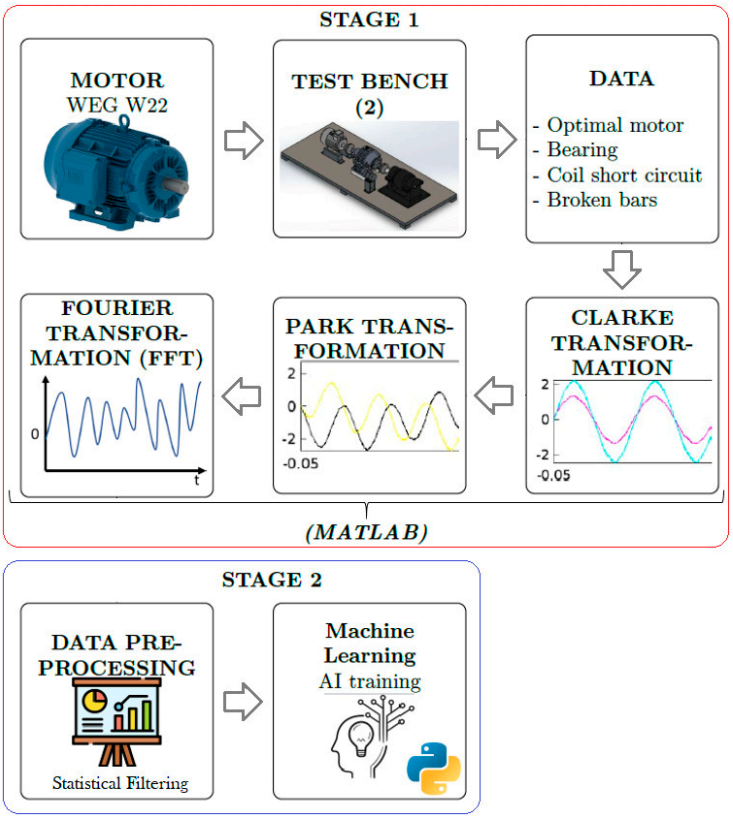


Figure 1. Stages of digital processing of the stator signals and training of the ML model.

Table 1. Motor and dynamometer specifications.

Motor WEG W22 High Eff		Magnetic Power Brake K&H MFG	
Characteristic	**Range**	**Characteristic**	**Specification**
Number of phases	3	Power supply	110/220 Vac, 50/60 Hz
Number of poles	4	Torque	0–9.999 Nm
Rated voltage	220/380–440 V	Speed sensor	60 pulses/rev optical sensor
Rated current	1.87/1.08–1.12 A	Torque sensor	Tensimeter
Power	0.37 kW–0.5 Hp	Temperature sensor	Thermal switch
Frequency	60 Hz	Cooling system	12 Vdc, 0.29 A
Speed	1700/1725 rpm	Brake controller	EM-3320-1N

The second stage covers training the Random Forest ML model on pre-processed data from four class types and validating the model.

2.1. Preliminary Concepts

The demands of today's market require a production facility equipped with Industry 4.0 enabling technologies, such as machine learning models, advanced statistics, mathematical tools, signal processing, and classical methods for identifying the condition of electric motors [15].

2.1.1. Emerging Failures

Emerging faults in a three-phase induction motor are defects or signs of deterioration that develop gradually; if not identified early, they can progress to more serious issues affecting the motor's performance, potentially leading to total failure and sudden production shutdowns. The main faults studied include voltage imbalance, insulation wear, rotor

misalignment, bearing deterioration, broken rotor bars, short circuits in the windings, and misaligned shafts.

Early detection of initial faults in three-phase induction motors enables preventive measures before issues escalate. This not only helps avoid unexpected outages and expensive damage in industrial processes but also boosts the operational productivity of technical staff and cuts down long-term maintenance expenses.

2.1.2. Mathematical Tools for Digital Signal Processing

The Clarke, Park, and Fourier transforms are considered essential tools in both mathematics and signal processing. These transforms are commonly applied in electrical engineering, especially in power system analysis and fault diagnosis of electrical machines.

- Clarke transform: Converts a three-phase system into a two-axis (α–β) system in a stationary plane, making the analysis of three-phase circuits and systems easier.
- Park transform: Converts variables of a three-phase system to a rotating reference coordinate system (d–q), simplifying the analysis of electrical machines and motor control.
- Fourier transform: Breaks down a signal into its frequency and amplitude parts, allowing analysis in the frequency domain, which is crucial for signal processing, spectral analysis, and fault diagnosis.

2.1.3. Advanced Statistics

Advanced statistical tools like the interquartile range, Tukey's method, and the Random Forest Classifier are vital for this case study because they facilitate data analysis, inferential statistics, and machine learning.

- Interquartile Range (IQR): This is a measure of central variability or an interval that contains 50% of the most representative data points in the sample; it is defined between the first quartile (Q1) and the third quartile (Q3).
- Tukey's Test: It facilitates exploratory data analysis by setting thresholds based on the IQR to identify outliers.
- Random Forest Classifier: This is a supervised model that belongs to the family of machine learning ensemble methods. It involves creating multiple decision trees (a forest) and combining their predictions to enhance accuracy and prevent overfitting.

2.2. Supervised Acquisition of Early-Stage Fault Data in a Three-Phase Motor

To take the measurements, the dynamometer controller was set to the motor's nominal operating parameters: a 220 V/60 Hz supply, delta connection, and a rated current of 1.87 A. The revolutions per minute (rpm) were increased manually using the magnetic brake controller until reaching the nominal speed of 1725 rpm.

Before acquiring the stator signals, they are conditioned using voltage-to-current transducers and signal amplifiers. This data is stored on an external device connected to the oscilloscope, where the motor behavior is recorded while simulating specific fault and normal operating conditions on the test bench. For each category, a set of 45 .csv files is compiled, containing 1000 digital samples for time and 3000 samples for the stator currents *ia*, *ib*, *ic*, totaling 720,000 digital samples across all four categories (Figure 2).

https://doi.org/10.3390/engproc2026154077

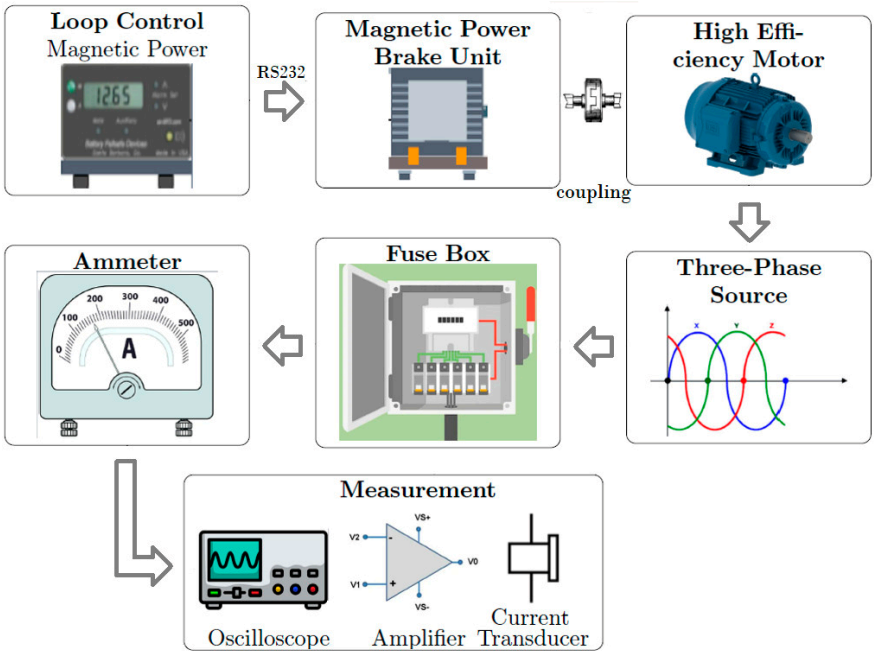


Figure 2. Signal acquisition process on a test bench.

2.3. Processing of Monitored Data

In line with the operating conditions of the electrical machines described above, this study uses an unstable system formulation (see Equations (1) and (2)), as this produces more realistic time-dependent results for the samples. This allows for more accurate real-time analysis of angles and visualization of the sinusoidal waves corresponding to the angles in each data set. It shows a similarity between α and I_1, and a 90° phase shift between β and α.

$$\alpha = \sqrt{\frac{2}{3}}\left(I_1 - \frac{1}{2}I_2 - \frac{1}{2}I_3\right) \tag{1}$$

$$\beta = \sqrt{\frac{2}{3}}\left(0 - \frac{\sqrt{3}}{2}I_2 - \frac{\sqrt{3}}{2}I_3\right) \tag{2}$$

In Figure 3, it is shown that the zero component indicates the cancellation of the three phases when the system is balanced, and the phase angle remains the same.

Due to the slip in the motor, Figure 3 of the Park transform shows that the two continuous signals change over time; these depend on the sampling period to obtain accurate and realistic calculations such as the operating frequency, instantaneous angular position θ(t), the magnetizing current (see Equation (3)), and the torque current (see Equation (4)).

$$\mathrm{d} = \alpha\cos(\theta) + \beta\sin(\theta) \tag{3}$$

$$\mathrm{q} = -\alpha\cos(\theta) + \beta\sin(\theta) \tag{4}$$

To convert the time-domain signals of the magnetization and torque currents into their frequency and amplitude components, the Fast Fourier Transform (FFT), an efficient implementation of the discrete Fourier transform, was used (Figure 4).

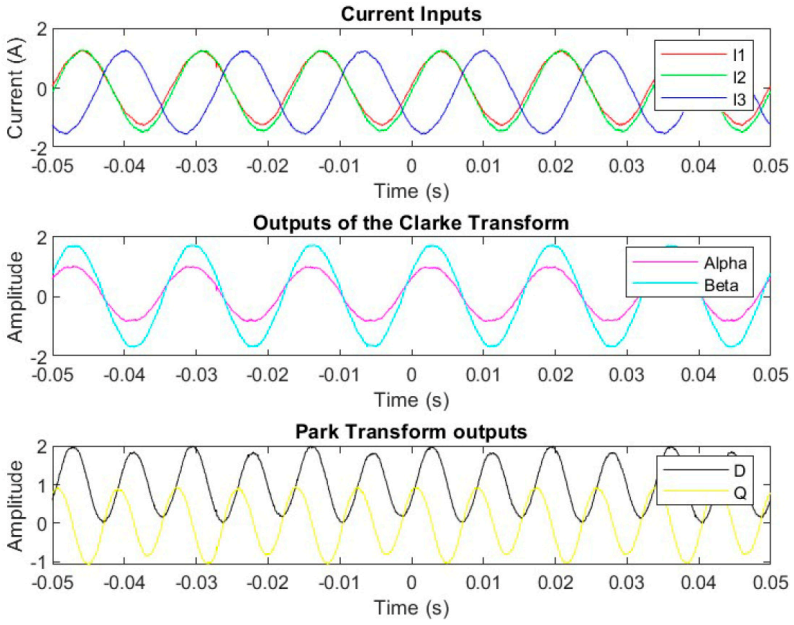


Figure 3. Clarke–Park transform.

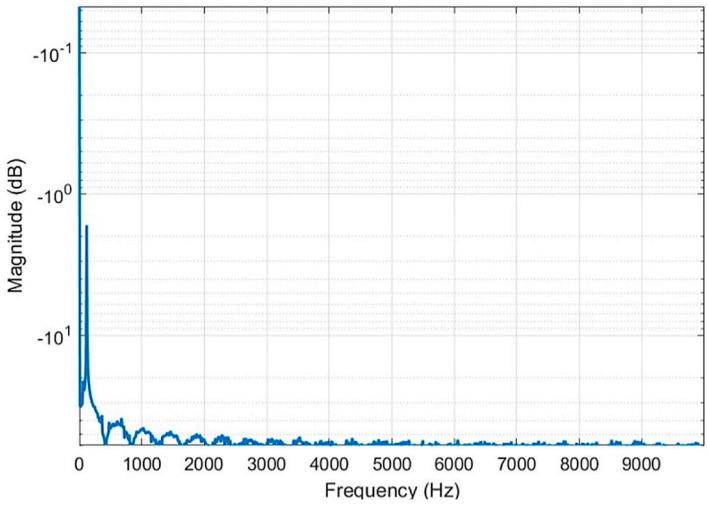


Figure 4. FFT applied to the magnetisation and torque currents.

2.4. Training Artificial Intelligence

The dataset used for training was stored in multiple .csv files, with columns containing spectral features from the FFT d, FFT q, and NaN error labels. A Python script was used to create the classification model, combining all the information into a single DataFrame.

To prevent outliers from skewing the standard deviation and shifting the mean, an interquartile range is chosen that allows the distribution to be refined while maintaining stability; therefore, an acceptable IQR is selected for the q-d components of the FFT across all classes (see Figure 5), filtering out outliers; this stabilizes the variance and removes transients. Additionally, through subsampling, the model is supplied with a balanced number of examples of each type for learning and classification, with equal weighting. In this way, a DataFrame is created containing pre-tabulated data from a dataset that corresponds to a single IQR.

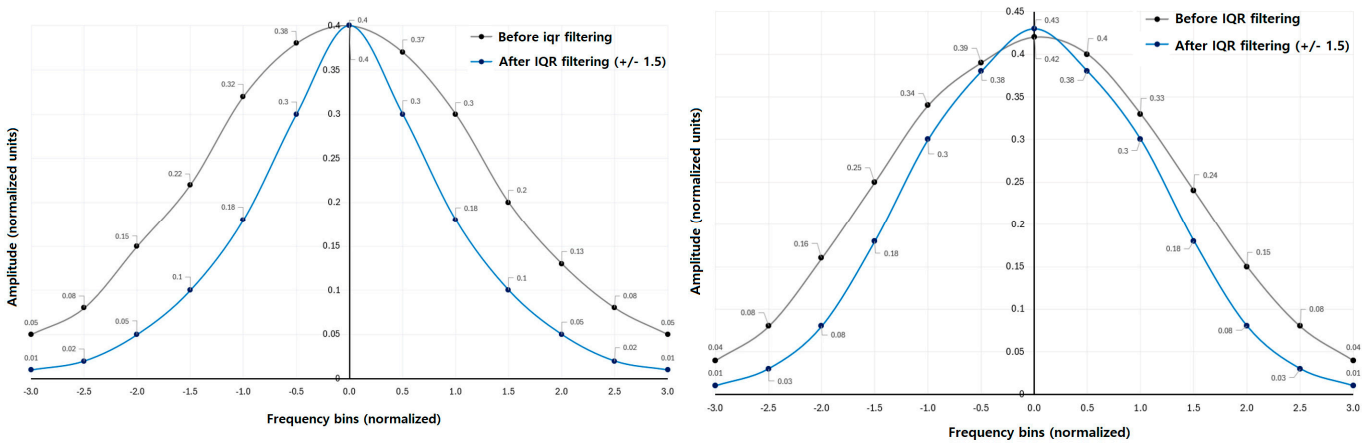


Figure 5. Data cleaning before and after filtering with ± IQR for the (**a**) FFT-d and (**b**) FFT-q components.

Based on the accuracy results and computational performance, this model was trained using the Random Forest Classifier algorithm with 100 estimators. Then, the model was assessed with a confusion matrix and a classification report to verify its accuracy and consistency.

3. Results

This section describes the behavior of the early-fault classification model used with three-phase induction motors, aimed at identifying four categories: bearing faults, short circuits, broken bars, and optimal operating conditions.

The ML algorithm was implemented using the scikit-learn library and integrated into the training model. The training was conducted in the Spyder Python IDE, creating 100 decision trees and setting 42 random modes to ensure reproducibility.

After applying mathematical transformations and normalization to each dataset, 36 .csv files were generated, each containing 3000 digital samples across frequency, torque, and magnetization, totaling 432,000 digital samples for the four categories, with outliers removed at approximately 40%. In total, 88.9% of this normalized data is used to train the ML model, while the remaining percentage is used to validate the classification system. The dataset consists of 16 .csv files, each with 12,000 samples per category.

To obtain the identification values for each category in the classification of torque and magnetization currents, they were assessed under eight different conditions, with the IQR tolerance varying across the following values: (±0.5, ±0.75, ±1.0, ±1.25, ±1.5, ±1.75, ±2.0, and ±2.25), as shown in Table 2.

As the tolerance value changes, the model struggles more to classify the test data accurately. This is clear in the percentages for bearing failure and optimal motor condition, where there is a lot of confusion between the two categories because their values are very similar. These results indicate that choosing the right IQR tolerance helps balance outlier removal with keeping important data for training the fault classification model.

From the table above, the results that significantly improve the classification model's accuracy are those using an interquartile range with a tolerance of 1.5.

After defining the IQR and refining thresholds with Tukey's method, the proportions of filtered data are identified as a distribution suitable for each class. Based on the data within IQR ±1.5, this subset shows that 49.7% of records belong to the CC loop class, 28.5% to patterns similar to the optimal class, 27.2% to the Broken Bar class, and 28.2% to the

Bearing class. This process ensures that the data fed into the model represents consistent patterns, thereby improving classification accuracy by approximately 14.7%.

Table 2. Classification results using different IQR thresholds.

Tolerance IQR	Category	Loop C.C. (%)	Optimum (%)	Rolling (%)	Broken Bar (%)
±0.5	CC in Lasso	41.2	18.4	17.8	22.6
	Optimal	16.2	22.5	25.3	36.0
	Broken Bar	18.0	20.4	25.3	36.3
	Bearing	19.3	22.0	24.5	34.2
±0.75	CC in Lasso	43.5	18.0	17.9	20.6
	Optimal	16.6	22.6	28.8	32.0
	Broken Bar	19.2	21.2	28.7	30.9
	Bearing	20.9	20.7	30.0	28.4
±1	CC in Lasso	47.9	17.7	17.6	16.8
	Optimal	20.7	27.5	27.1	24.7
	Broken Bar	23.2	24.0	27.4	25.4
	Bearing	24.4	22.2	30.0	23.4
±1.25	CC in Lasso	46.2	16.9	16.8	20.1
	Optimal	16.9	27.0	26.6	29.5
	Broken Bar	19.6	25.2	26.3	28.9
	Bearing	22.4	23.0	27.8	26.8
±1.5	CC in Lasso	49.7	17.2	17.7	15.4
	Optimal	18.7	28.5	26.0	26.8
	Broken Bar	20.7	26.3	25.8	27.2
	Bearing	23.0	24.5	28.2	24.3
±1.75	CC in Lasso	48.4	17.4	18.0	16.2
	Optimal	19.1	27.1	28.6	25.2
	Broken Bar	20.7	23.4	29.6	26.3
	Bearing	22.3	22.4	31.5	23.8
±2	CC in Lasso	50.6	17.0	15.8	16.6
	Optimal	19.5	28.2	28.1	24.2
	Broken Bar	23.5	24.9	25.9	25.7
	Bearing	24.8	23.1	28.4	23.7
±2.25	CC in Lasso	48.0	16.6	19.7	15.7
	Optimal	18.3	27.3	29.4	25.0
	Broken Bar	20.9	23.1	29.6	26.4
	Bearing	23.5	21.8	29.5	25.2

Furthermore, the classification model was validated using the confusion matrix, which is normalized by the total number of samples, indicating that the system achieves over 97% accuracy across all categories (see Figure 6). A slight confusion between the Optimal and Bearings classes suggests near-spectral similarity, while the CC classes in Loop and Broken Bar are detected with 99% reliability. This indicates that there are intrinsic spectral characteristics in these data that favorably influence the model's performance, enabling highly accurate classification.

The ML model demonstrated highly consistent performance in fault detection. For the "DC in Loop" category, it achieved a value of 0.99, whilst for the "Optimal" condition, performance was 0.97; for the "Bearing" condition, a value of 0.978 was obtained; and finally, for the "Broken Bar" condition, a value of 0.99 was achieved. This resulted in an overall accuracy of 98.25%.

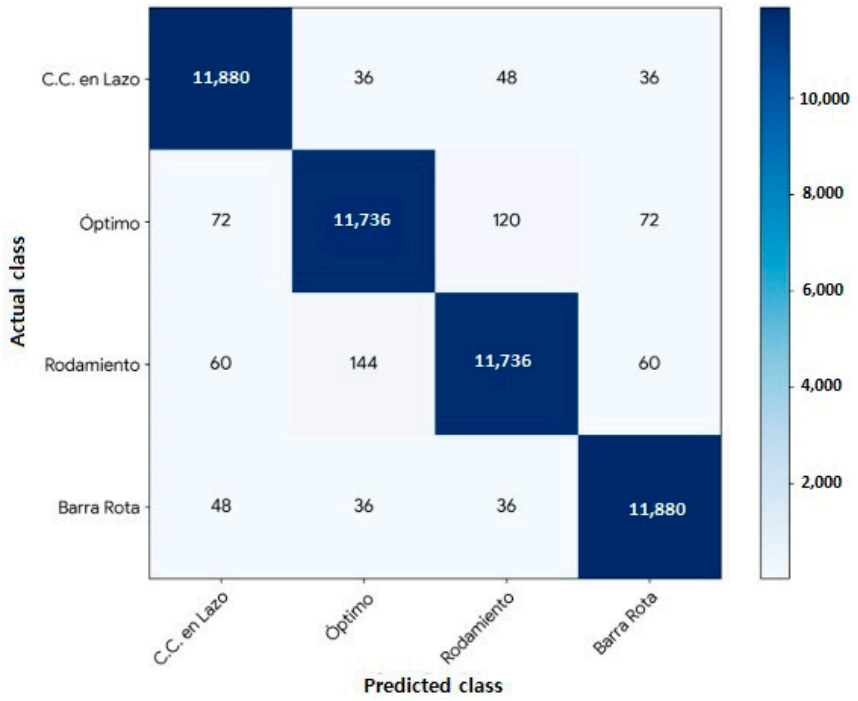


Figure 6. Performance of the Random Forest algorithm in the diagnosis of four class categories.

Additionally, the implementation of IQR filtering and its adjustment for data cleansing were evaluated using the same methodology as that applied to mathematical transformations. For this analysis, the established threshold of 1.5± was modified by applying two alternative values: ±1.25 and ±1.75. The results showed that the model's overall accuracy decreased in both cases by an average of 84.2%, highlighting the sensitivity of performance to variations in statistical parameters during the pre-processing and validation stages.

4. Discussion

The issues related to unplanned production stops, financial losses, and the pressures from both national and international competition demand effective technical and methodological solutions. A review of the literature shows proposals aimed at addressing this problem, including methodologies like the classical approach, which requires specialized personnel for signal analysis; the use of statistical analysis tools; and traditional and robust methods combined with various types of ML models for identifying specific faults. However, a gap exists between the high accuracy of models focused on a single fault and the inconsistent results of studies that try to address multiple faults at once. Additionally, although recent research is innovative, it often stays at a conceptual level without providing a clear, applicable, and reproducible technical methodology for real industry applications.

In this regard, this study is designed as an extension of those works that combine mathematical transforms, statistical analysis, and AI to expand the diagnostic approach to a multi-fault strategy. The development of this diagnostic system for detecting incipient motor faults begins with collecting data from the motor operating under normal conditions. Signal processing was performed sequentially using the Clarke, Park, and FFT transforms; the resulting data were then normalized and classified into four conditions (Loop CC, Rolling, Broken Bar, and Optimal). This dataset was used to train the Random Forest Classifier machine learning model. Using this methodology, the model validation achieved an overall diagnostic accuracy of over 98%.

During validation tests, a percentage of false positives was identified, which decreased the model's accuracy. In response, the number of .cvs files was increased by 12.5%, achiev-

ing acceptable accuracy for each class. Furthermore, to prevent distortions in the training data and potential normal deviations, it was decided to incorporate the Park transform into the signal processing.

Although diagnosing early faults is part of predictive maintenance, it remains a particular challenge that requires further research. Looking ahead, it is suggested to explore more on detecting early signs of degradation by using mathematical transformations, statistical analysis, and machine learning models to improve predictive maintenance's ability to forecast critical faults in induction motors.

The slight ambiguity between the "Optimal" and "Bearing" classes suggests that the stationary spectral features extracted using the fast Fourier transform (FFT) may show limited separability during early bearing degradation. Future work could explore time-frequency approaches, such as the discrete wavelet transform (DWT) or the wavelet packet transform (WPT), which have demonstrated greater sensitivity to the non-stationary transient components associated with bearing-related failures.

Although the proposed IQR threshold proved robust under controlled laboratory conditions, industrial environments may introduce additional variability due to dynamic load changes and operational fluctuations. Future work could evaluate adaptive thresholding strategies in real-world industrial settings.

5. Conclusions

The analysis of operating modes and fault conditions in three-phase induction motors evaluates the effectiveness of the classification model in detecting early-stage anomalies. Implementing pre-processing based on the interquartile range standardized input patterns and simplified algorithm training. This organization of categorical data, including Optimal, Bearings, Loop CC, and Broken Bar conditions, greatly improved the system's ability to distinguish among the different classes.

From a technical standpoint, the Random Forest Classifier was ideal for this supervised data environment. Since it is a parallel ensemble model, it does not require neural network parameters like learning rate or epochs, which saves computation time without sacrificing diagnosis robustness. Using subsampling and statistical validation tools helped eliminate noise, leading to a classification that significantly reduces false positives and negatives.

In summary, selecting highly discriminatory features has created a diagnostic system with better detection abilities, capable of functioning effectively in industrial environments. Future research should aim to reduce remaining classification ambiguity to shift from reactive detection to predictive maintenance that maintains operational continuity and the reliability of key assets.

Author Contributions: Conceptualization, W.O.; methodology, A.V., M.P. and E.Y.; software, A.V. and E.Y.; validation, M.P., E.Y. and W.O.; formal analysis, W.O.; investigation, W.O., A.V. and E.Y.; resources, A.V., E.Y. and M.P.; data curation, A.V. and E.Y.; writing—original draft preparation, W.O. and M.P.; writing—review and editing, W.O.; visualization, W.O.; supervision, W.O.; project administration, W.O. All authors have read and agreed to the published version of the manuscript.

Funding: The APC was funded by Universidad Politécnica Salesiana (UPS). This research received no external funding for its execution.

Institutional Review Board Statement: Not applicable.

Informed Consent Statement: Not applicable.

Data Availability Statement: The data supporting the findings of this study are included within the article. Further inquiries can be directed to the corresponding author.

Acknowledgments: This work was supported by UPS.

Conflicts of Interest: The authors declare no conflicts of interest.

References

1. Javed, M.R.; Shabbir, Z.; Asghar, F.; Amjad, W.; Mahmood, F.; Khan, M.O.; Virk, U.S.; Waleed, A.; Haider, Z.M. An Efficient Fault Detection Method for Induction Motors Using Thermal Imaging and Machine Vision. *Sustainability* **2022**, *14*, 9060. [CrossRef]
2. Araújo, V.G.d.; Bissiriou, A.O.-S.; Villanueva, J.M.M.; Villarreal, E.R.L.; Salazar, A.O.; Teixeira, R.d.A.; Fonsêca, D.A.d.M. Monitoring and Diagnosing Faults in Induction Motors' Three-Phase Systems Using NARX Neural Network. *Energies* **2024**, *17*, 4609. [CrossRef]
3. Sabah, A.N.; Jaffery, Z.A. Fault Detection of Induction Motor Using Thermal Imaging. In Proceedings of the 2022 IEEE IAS Global Conference on Emerging Technologies (GlobConET), Arad, Romania, 20–22 May 2022; pp. 84–90. [CrossRef]
4. Al-Musawi, A.K.; Anayi, F.; Packianather, M. Three-phase induction motor fault detection based on thermal image segmentation. *Infrared Phys. Technol.* **2020**, *104*, 103140. [CrossRef]
5. Enejo, I.S.; Adegboye, B.; Imoru, O.; James, T.O. Fault Diagnosis in a Three-Phase Induction Motor Using Enhanced Park Vector Approach. In Proceedings of the 2022 IEEE Nigeria 4th International Conference on Disruptive Technologies for Sustainable Development (NIGERCON), Lagos, Nigeria, 5–7 April 2022; pp. 1–6. [CrossRef]
6. Cruz, S.M.A.; Cardoso, A.J.M. Stator winding fault diagnosis in three-phase synchronous and asynchronous motors by the extended Park's vector approach. *IEEE Trans. Ind. Appl.* **2001**, *37*, 1227–1233. [CrossRef]
7. Garcia-Calva, T.; Morinigo-Sotelo, D.; Fernandez-Cavero, V.; Romero-Troncoso, R. Early Detection of Faults in Induction Motors—A Review. *Energies* **2022**, *15*, 7855. [CrossRef]
8. Kumar, R.; Anand, R. Application of Park's Vector and Current Envelope Method for Diagnosis of Stator Winding Inter Turn Fault of Induction Motors. In Proceedings of the 2023 7th International Conference on Green Energy and Applications (ICGEA), Singapore, 10–12 March 2023; pp. 168–174. [CrossRef]
9. Oo, A.T.; Mon, A.; Tun, M.Z. Induction Motor Fault Detection and Classification System Using Proposed Fusion Features and Machine Learning Techniques. In Proceedings of the 2024 26th International Conference on Digital Signal Processing and Its Applications (DSPA), Moscow, Russia, 27–29 March 2024; pp. 1–6. [CrossRef]
10. Osornio-Rios, R.A.; Cueva-Perez, I.; Alvarado-Hernandez, A.I.; Dunai, L.; Zamudio-Ramirez, I.; Antonino-Daviu, J.A. FPGA-Microprocessor Based Sensor for Faults Detection in Induction Motors Using Time-Frequency and Machine Learning Methods. *Sensors* **2024**, *24*, 2653. [CrossRef] [PubMed]
11. Priyandoko, G.; Siswanto, D.; Istiadi, I.; Effendi, D.U.; Naufal, E.R. Bearing Fault Detection Using Discrete Wavelet Transform and Partitioning Around Medoids Methods. *Lect. Notes Electr. Eng.* **2022**, *730*, 219–226. [CrossRef]
12. Goh, Y.-J.; Kim, K.-M. Clarke-Park Transformation-Based Input Configuration for CNN Diagnosis of Stator Faults in Three Phase Induction Motors Using Motor Current Signature Analysis. *IEEE Access* **2025**, *13*, 150505–150516. [CrossRef]
13. Rengifo, J.; Moreira, J.; Vaca-Urbano, F.; Alvarez-Alvarado, M.S. Detection of Inter-Turn Short Circuits in Induction Motors Using the Current Space Vector and Machine Learning Classifiers. *Energies* **2024**, *17*, 2241. [CrossRef]
14. Halder, S.; Bhat, S.; Zychma, D.; Sowa, P. Broken Rotor Bar Fault Diagnosis Techniques Based on Motor Current Signature Analysis for Induction Motor—A Review. *Energies* **2022**, *15*, 8569. [CrossRef]
15. Osornio, C.; Alfredo, J.R.; Saucedo, J.; Morales, H. Método para la Detección de Fallos en los Rodamientos Mediante Flujo Magnético y la Aplicación de la Transformada de Fourier. *Rev. Acad. J. Puebla* **2022**, *14*, 231–236.

Disclaimer/Publisher's Note: The statements, opinions and data contained in all publications are solely those of the individual author(s) and contributor(s) and not of MDPI and/or the editor(s). MDPI and/or the editor(s) disclaim responsibility for any injury to people or property resulting from any ideas, methods, instructions or products referred to in the content.